Figure S1: 3 day back trajectories for the B762 science period. Back trajectory analyses were calculated at 30 second intervals along each flight path using the National Oceanic and Atmospheric Administration HYbrid Single-Particle Lagrangian Integrated Trajectory (NOAA HYSPLIT 4.0) model (Draxler and Hess 1998), as described in Liu et al. (2015) and Young et al. (2016). GDAS reanalysis meteorology (Global Data Assimilation System; NOAA Air Resources Laboratory, Boulder, CO, USA) was used to simulate the 3D wind fields; however, turbulent motions are not resolved by the model and therefore some uncertainty is attached to the modelled trajectories (Fleming et al. 2012). A sample of trajectories modelled over the sea ice (red), MIZ (magenta) and ocean (blue) are shown. Sea ice concentration from the NSIDC is shown in colour, with the ocean and sea ice depicted in blue and yellow respectively. Sea ice data at the north pole are not included.

# References

R. R. Draxler and G. D. Hess. An Overview of the HYSPLIT_4 Modelling System for Trajectories, Dispersion, and Deposition. Australian Meteorological Magazine, 47:295–308, 1998.

Z. L. Fleming, P. S. Monks, and A. J. Manning. Review: Untangling the influence of air-mass history in interpreting observed atmospheric composition. Atmospheric Research, 104:1–39, February 2012. doi: 10.1016/j.atmosres.2011.09.009.

D. Liu, Quennehen, E. Darbyshire, J. D. Allan, P. I. Williams, J. W. Taylor, B. Bauguitte, S. J., M. J. Flynn, M. W. Gallagher, K. N. Bower, T. W. Choularton, and H. Coe. The importance of Asia as a source of black carbon to the European Arctic during springtime 2013. Atmospheric Chemistry & Physics, 15:1484314887, 2015. doi: doi:10.5194/acpd-15-14843-2015.

G. Young, H. M. Jones, E. Darbyshire, K. J. Baustian, J. B. McQuaid, K. N. Bower, P. J. Connolly, M. W. Gallagher, and T. W. Choularton. Size-segregated compositional analysis of aerosol particles collected in the european arctic during the accacia campaign. Atmospheric Chemistry and Physics, 16(6):4063–4079, 2016. doi: 10.5194/acp-16-4063-2016.
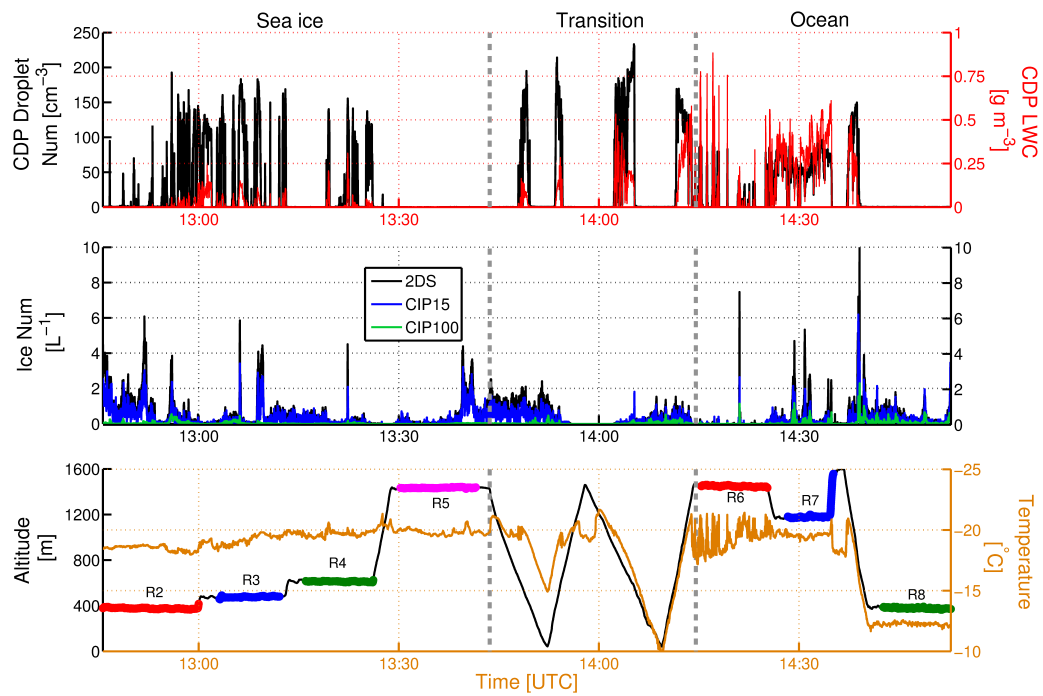
Figure S2: Time series of data collected during the science period of ACCACIA flight B762. **Top row:** CDP droplet number concentration (black) and derived liquid-water content (red). **Second row:** 2DS (black), CIP15 (blue) and CIP100 (green) ice number concentration. **Bottom row:** GPS altitude (black), with individual SLRs noted in colour, and temperature measured by the Rosemount de-iced temperature sensor (orange). SLR colours relate to data shown in Figs. 5 and 7. Sea ice, transition and ocean regions are indicated above the top row.
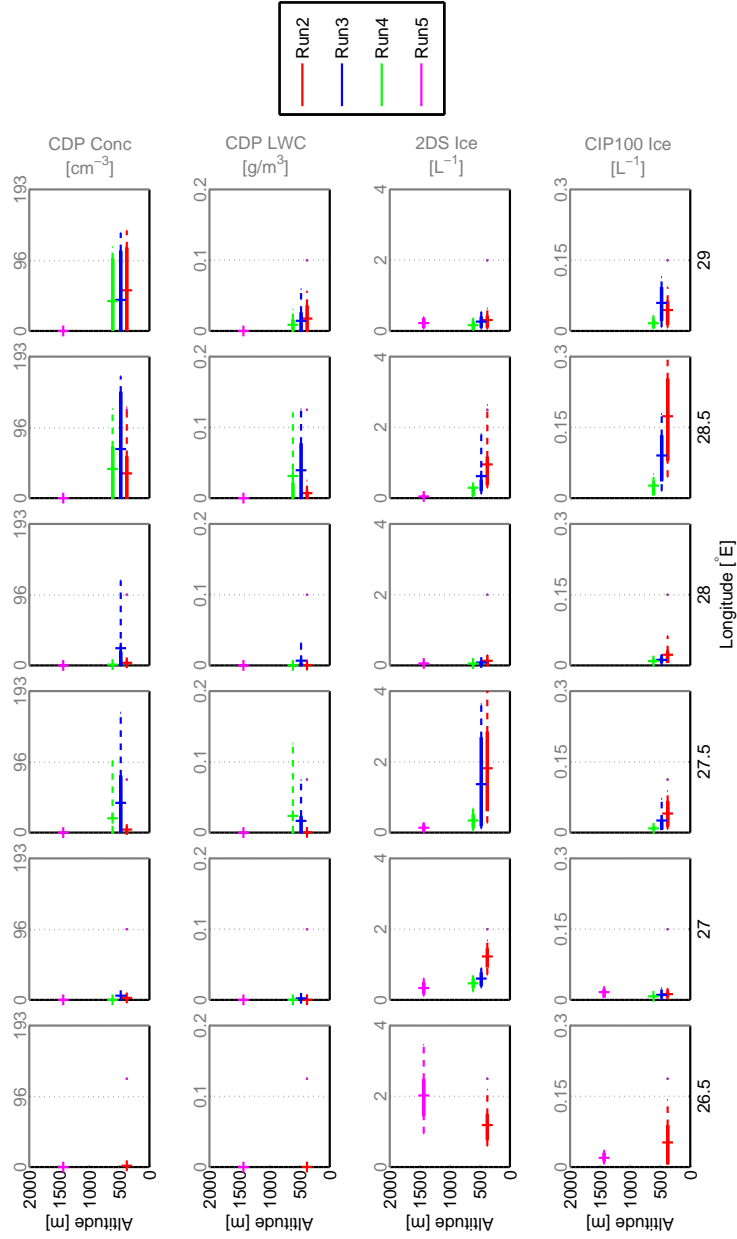
Figure S3: Percentile plots of CDP droplet number concentration (**top row**), CDP liquid-water content (**second row**), 2DS ice number concentration (**third row**) and CIP100 ice number concentration (**bottom row**) measured over the sea ice. Each column represents a different longitude bin, therefore the figure can be viewed as being from west to east from left to right. The boxes are coloured differently dependent on the SLR at which the data was measured, as indicated in the legend. The inhomogeneous structure of the cloud spatially is clear from the variation between longitude bins.
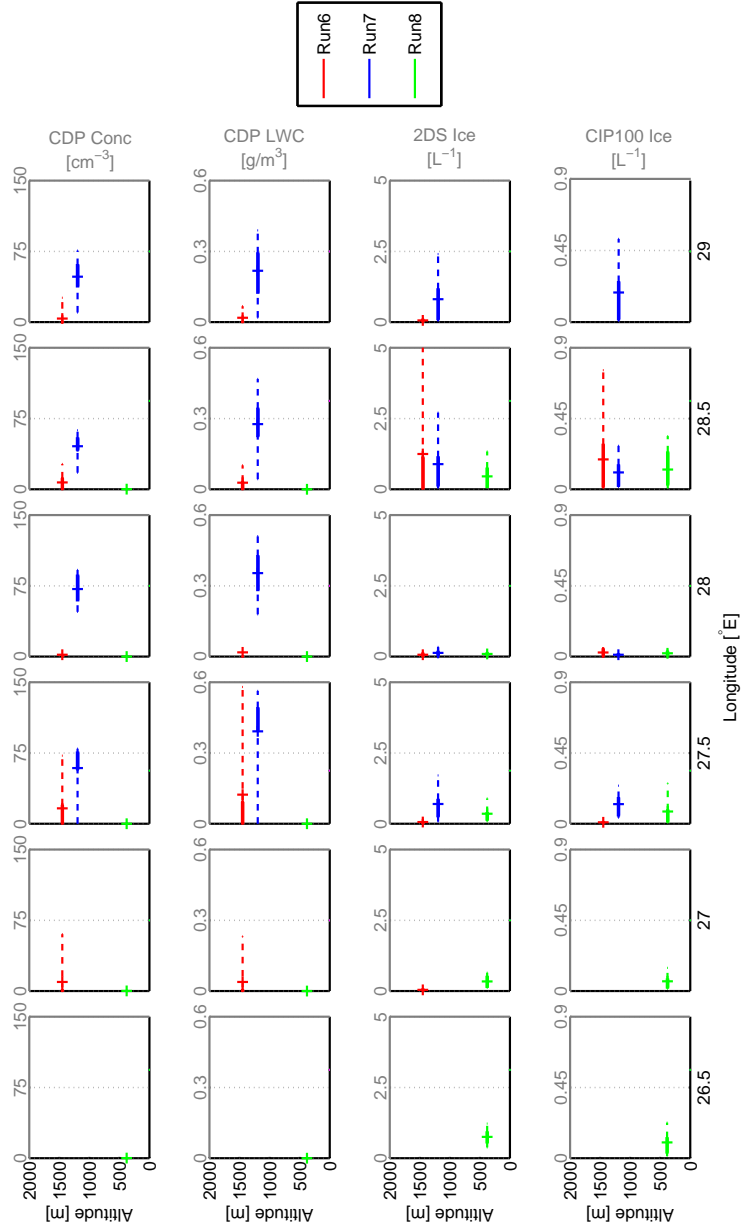
Figure S4: Percentile plots of CDP droplet number concentration (**top row**), CDP liquid-water content (**second row**), 2DS ice number concentration (**third row**) and CIP100 ice number concentration (**bottom row**) measured over the ocean. As in Fig. S3, columns represent different longitude bins and data are coloured by SLR (as shown in the legend). The cloud is more homogeneous than the sea ice case; however, some spatial variability is still noted.

14:57:51.066-64721
14:57:47.049-64330
14:57:41.055-63938
14:57:37.000-63506
14:57:20.053-63138
14:54:55.058-62546
14:54:02.091-62110
14:53:38.091-61841
14:53:33.078-61539
14:53:26.010-60996
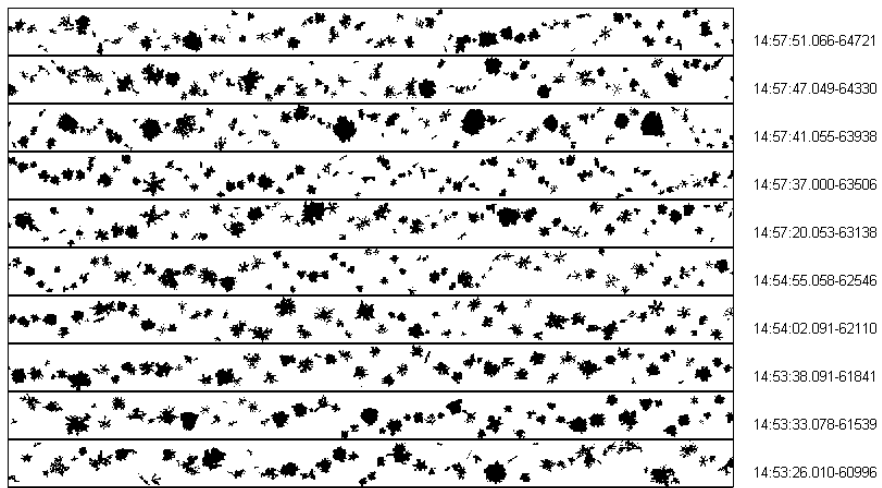
Figure S5: Example data from the CIP100 at cloud base over the ocean. Large dendrites are observed, with potential shattering events noted. Vertical width of image strip represents a size range of 6.4 mm.